

Effective pair potential reproducing the measured structure factor of liquid Cu near the melting point

This article has been downloaded from IOPscience. Please scroll down to see the full text article.

1991 J. Phys.: Condens. Matter 3 7475

(<http://iopscience.iop.org/0953-8984/3/38/019>)

View [the table of contents for this issue](#), or go to the [journal homepage](#) for more

Download details:

IP Address: 171.66.16.147

The article was downloaded on 11/05/2010 at 12:34

Please note that [terms and conditions apply](#).

Effective pair potential reproducing the measured structure factor of liquid Cu near the melting point

Takashi Arai and Isao Yokoyama

Department of Mathematics and Physics, National Defense Academy, Yokosuka 239, Japan

Received 30 May 1991

Abstract. An effective pair potential for liquid Cu at 1423 K has been obtained from small-angle structure factor data with the help of inverse power potentials to describe the structure factors in the high-wavenumber region. This effective pair potential indicates a marked difference, in position and depth of the first minimum, from the interatomic potential derived from first principles. The experimental structure data, from well below the first peak to high wavenumber, can be reproduced by a molecular dynamics simulation using the present effective pair potential. The molecular dynamics results for the pair distribution function, the specific heat at constant volume, the self-diffusion constant and the shear viscosity coefficient are also presented in comparison with the experimental data.

1. Introduction

The direct determination of the effective pair potential $v_{\text{eff}}(r)$ from the measured structure factor $a(k)$ of a liquid has been a continuing interest since the pioneering works of Johnson and March (1963) and Johnson *et al* (1964). Up to now, many different schemes, all approximate to some degree, have been proposed for this purpose. An article written by March (1987) has surveyed recent progress in this respect, which concludes that a procedure is now available for the inversion of structure data that is quantitatively reliable, given really accurate experimental structure data over a very wide range of wavenumber k including, in a very essential way, small-angle scattering data.

An inversion scheme that has been proposed by one of the authors (Naito and Yokoyama 1985) focuses on the low- k region and appears to be competitive in accuracy with those employed hitherto. This approach has been successfully applied to liquid Na and K near their melting points and to expanded liquid Rb for temperatures up to 1900 K (Naito and Yokoyama 1988, 1989). The elaborate low-angle scattering experiments recently performed by Waseda and Ueno (1987) have made it possible to extend this method even to liquid Fe (Arai *et al* 1988, 1990b) and Cu (Arai *et al* 1990a) for obtaining the tail part of $v_{\text{eff}}(r)$.

The purpose of the present paper is as follows: first, to show the $v_{\text{eff}}(r)$ obtained in this study, comparing it with the interatomic potential derived entirely from first principles for solid Cu by Lam *et al* (1983); second, to examine, using molecular dynamics, whether or not this $v_{\text{eff}}(r)$ can reproduce the low- k diffraction data by which this $v_{\text{eff}}(r)$

is extracted; third, to recalculate some physical quantities so as to compare with those obtained in the previous work on liquid Cu.

Instead of using the so-called integral equations employed by many workers, we invoke the Monte Carlo simulation results by Hansen and Schiff (1973, and references therein) and use the liquid phonon theory (Bratby *et al* 1970, March and Tosi 1976, Naito and Yokoyama 1985) which applies to the low- k region of $a(k)$. The present inversion scheme, though not so sophisticated as the recent refined-structural theories (March 1987, March 1990), works very well for obtaining information regarding the attractive part of $v_{\text{eff}}(r)$, of which we know virtually nothing for liquid noble and transition metals.

In section 2 we describe the model. In section 3 we indicate the basis of our analysis. In section 4 we outline the molecular dynamics calculations. Our results and discussions, including our previous results on liquid Cu, are given in section 5. We end, in section 6, with some conclusions drawn from the present studies.

2. The model

In previous works we supposed that $v_{\text{eff}}(r)$ can be divided into two parts:

$$v_{\text{eff}}(r) = v_{\text{core}}(r) + v_{\text{tail}}(r) \quad (1)$$

where $v_{\text{core}}(r)$ denotes a positive repulsive potential to represent the core part and is mainly responsible for the $a(k)$ at large k , while $v_{\text{tail}}(r)$ denotes the tail potential and is responsible for modifications at small k . Then we took an inverse power potential or a repulsive Yukawa potential as the core potential. In liquid alkali metals the $a(k)$ beyond the first peak can be well described by a single repulsive potential. In liquid Fe and Cu, however, we found that any repulsive potential cannot describe the height of the first peak correctly, although the description of the $a(k)$ beyond the first peak is good enough to warrant the assumption (Arai *et al* 1988, 1990a, b). In this study we modify equation (1) in order to include an attractive potential as

$$v_{\text{eff}}(r) = v_{\text{ref}}(r) + v_{\text{tail}}(r) \quad (2)$$

and

$$v_{\text{ref}}(r) = v_{\text{core}}(r) + v_{\text{attr}}(r) \quad (3)$$

where $v_{\text{ref}}(r)$ denotes a reference potential and $v_{\text{attr}}(r)$ is an attractive potential which is assumed to control the first-peak height of the $a(k)$. Since the tail potential $v_{\text{tail}}(r)$ in our model is given from the random phase approximation it is responsible only for the $a(k)$ at low k and does not affect the height of the first peak. Equations (2) and (3) lead to equation (1) by setting $v_{\text{attr}}(r)$ to zero. Thus once a $v_{\text{ref}}(r)$ is determined to reproduce diffraction data from first-peak region to high k , the $v_{\text{tail}}(r)$ is evaluated from the small-angle part of the diffraction data as

$$v_{\text{tail}}(r) = \frac{k_{\text{B}} T}{(2\pi)^3 \rho} \int_0^{k_0} \left(\frac{1}{a_{\text{expt}}(k)} - \frac{1}{a_{\text{ref}}(k)} \right) \frac{\sin kr}{kr} 4\pi k^2 dk \quad (4)$$

where $k_0 = (18\pi^2 \rho)^{1/3}$ with ρ being the number density of ions, and $a_{\text{expt}}(k)$ and $a_{\text{ref}}(k)$ are, respectively, the experimental structure factor and the reference structure factor

corresponding to the $v_{\text{ref}}(r)$. Of course, the fit for $k \geq k_0$ is not perfect because we have a sum rule:

$$\int_0^{\infty} (a_{\text{expt}}(k) - a_{\text{ref}}(k)) 4\pi k^2 dk = 0. \quad (5)$$

However, we shall neglect any imperfection in the fit in this region and concentrate instead on the small- k , large- r regions.

3. Procedure

First, a $v_{\text{core}}(r)$, the main part of a $v_{\text{eff}}(r)$, is chosen to describe an $a_{\text{expt}}(k)$ in the high- k region. The Yukawa-type potential (Hayter and Penfold 1981, Hayter *et al* 1983) is convenient for this purpose, but in the case of liquid Cu at 1423 K the inverse power potential r^{-12} gives a better description of the $a_{\text{expt}}(k)$ (Waseda 1980). Therefore we choose the r^{-12} potential as the $v_{\text{core}}(r)$ as in the previous work on liquid Cu:

$$v_{\text{core}}(r) = \varepsilon(\sigma/r)^{12} \quad (6)$$

where the values of ε and σ are 0.007875 au and 2.3658 Å, respectively (Hansen and Schiff 1973, and references therein). The corresponding $a_{\text{core}}(k)$ is shown in figure 1 together with $a_{\text{expt}}(k)$.

Second, in order to reduce the first-peak height of $a_{\text{core}}(k)$ shown in figure 1(a) a negative inverse power potential $-\varepsilon(\sigma/r)^n$ is employed as $v_{\text{attr}}(r)$. The values of 4, 6 and 8 for n are tested in combination with the $v_{\text{core}}(r)$ given in equation (6). We expect that $v_{\text{attr}}(r)$ will affect the first-peak height including the low- k region considerably, without changing the quality of description of the $a(k)$ in the high- k region. Thus we can determine $v_{\text{ref}}(r)$. By the use of this $v_{\text{ref}}(r)$, a molecular dynamics simulation is carried out to obtain the $a_{\text{ref}}(k)$ which is, without recourse to Fourier transformation of the pair distribution function, calculated from the following definition

$$a(k) = \frac{1}{N} \left\langle \left| \sum_j^N \exp(ik \cdot r_j) \right|^2 \right\rangle. \quad (7)$$

Here N is the number of particles, r_j the position of the particle j and the angular brackets denote the statistical average. In the calculation of $a(k)$ this is averaged over 800 time steps.

$v_{\text{tail}}(r)$ is then evaluated from equation (4) and this is used in equation (2) to obtain $v_{\text{eff}}(r)$. Using this $v_{\text{eff}}(r)$, the corresponding $a(k)$ is again calculated using equation (7).

4. Molecular dynamics calculations

A microcanonical molecular dynamics (NVE molecular dynamics, see Verlet 1967) is used to calculate the structure factors, the pair distribution functions, the specific heats at constant volume, the self-diffusion constants and the shear viscosity coefficients. These physical quantities are also computed, for comparison, using the interatomic pair potential derived from *ab initio* calculations (Lam *et al* 1983). A more realistic molecular dynamics with constant-temperature and/or constant-pressure algorithms is favourable, but the NVE molecular dynamics is faster to run, and hence more convenient for the

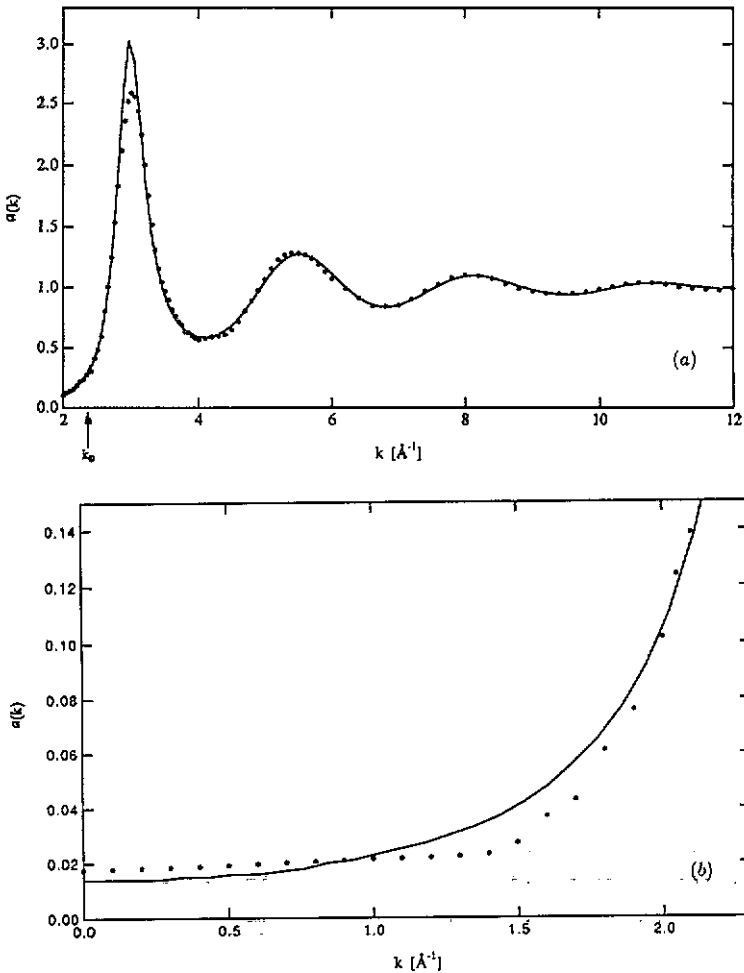


Figure 1. Structure factors for (a) the high- k region, (b) the low- k region: —, Monte Carlo simulation results $a_{\text{core}}(k)$ (Hansen and Schiff 1973); ●, experimental data $a_{\text{expt}}(k)$ (Waseda 1980, Waseda and Ueno 1987).

present purpose. Throughout this work the simulations are carried out under the following conditions:

- (i) three-dimensional periodic boundary conditions are used;
- (ii) the number of particles $N = 1000$;
- (iii) the initial configuration is simple cubic lattice;
- (iv) the temperature is set to be 1423 K;
- (v) the density is fixed at 7.97 g cm^{-3} ;
- (vi) the time unit is $5 \times 10^{-15} \text{ s}$;
- (vii) the annealing step is 5000 times.

The potentials used are not cut off so that half the length of the box size L is the maximum distance. Therefore the smallest length of k in the calculated structure factors becomes $2\pi/L$. For a few thousand steps during annealing, temperature is maintained in the set

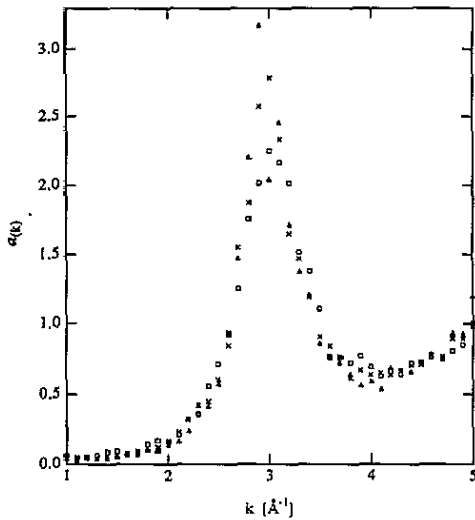


Figure 2. Structure factors for reference potentials in the first-peak region; Δ , $v_{\text{ref}}(r) = \epsilon(\sigma/r)^{12} - \epsilon(\sigma/r)^4$; \times , $v_{\text{ref}}(r) = \epsilon(\sigma/r)^{12} - \epsilon(\sigma/r)^6$; \square , $v_{\text{ref}}(r) = \epsilon(\sigma/r)^{12} - \epsilon(\sigma/r)^8$. These are obtained by averaging over 200 time steps so that a scatter of data is seen in the figure.

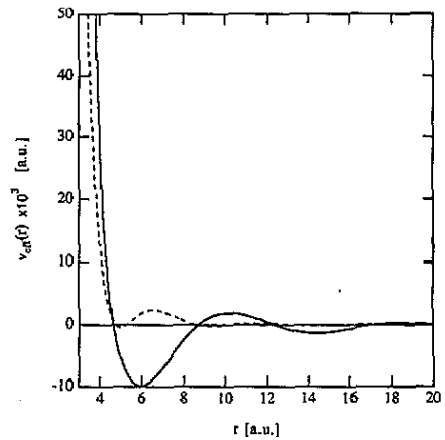


Figure 3. Effective pair potentials: —, the present work; ---, first-principles interatomic potential (Lam *et al* 1983).

value. However, since the specific heat at constant volume is calculated from the fluctuations in the kinetic temperature of the system the constraint on temperature is not used for this quantity. The self-diffusion constant is evaluated via the velocity autocorrelation function (Hansen and McDonald 1986). The shear viscosity coefficient is calculated by the correlation function based on the Kubo–Green formula (Berezhkovsky *et al* 1984, Hansen and McDonald 1986).

5. Results and discussions

5.1. Structure factor and effective pair potential

To determine a suitable $v_{\text{eff}}(r)$ three kinds of $v_{\text{attr}}(r)$ were tested with $n = 4, 6$ and 8 . The results are shown in figure 2. As can be seen from figure 2, the first-peak height of the $a(k)$ decreases with increasing number of inverse power without significant changes to the description at high k . We employ $-\epsilon(\sigma/r)^6$ as the $v_{\text{attr}}(r)$ in this work since this gives the right size of the first-peak height. Of course, there might exist a better $v_{\text{attr}}(r)$ than this choice, but it is not essential for the purpose of the present study. It should be noticed that this $v_{\text{ref}}(r)$ is different, in the definitions ϵ and σ , from the conventional Lennard-Jones potential. Since the values of ϵ and σ have been determined by the crystallization conditions for the inverse power potentials (Hansen 1970, Hoover *et al* 1971) the direct use of these values is not always correct in the case of liquid Cu at 1423 K. However, we assume the conceivable errors to be negligible.

The effective pair potential $v_{\text{eff}}(r)$ obtained from equation (2) is illustrated in figure 3 in comparison with the interatomic potential derived from first principles (Lam *et al* 1983). The $v_{\text{eff}}(r)$ obtained in this work is quite different in the position of the first

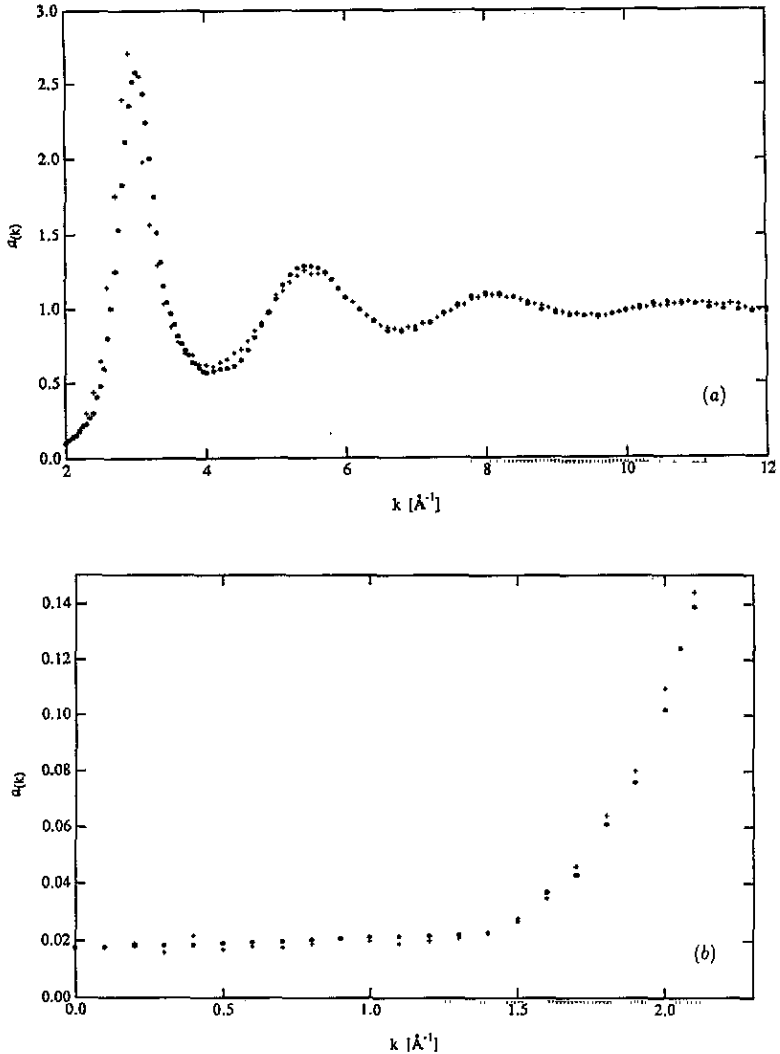


Figure 4. Structure factors of liquid Cu at 1423 K: \bullet , experimental data (Waseda 1980, Waseda and Ueno 1987); $+$, for present potential. (a) denotes the high- k region, and (b) the low- k region. The present results are obtained by averaging over 800 time steps.

minimum from the first-principles interatomic potential. Our potential is characterized by a deep attractive part followed by rather long-ranged oscillations. Thus our interest is focused on the following questions. First, does our potential reproduce the low- k diffraction data by which this potential is extracted? Second, is our potential suitable for predicting physical properties of liquid Cu? To answer the first question we show, in figures 4 and 5, the structure factors computed from equation (7) using the two potentials shown in figure 3. As can be seen from figure 4(a), the $a_{\text{exp}}(k)$ are quite well reproduced by the molecular dynamics calculations except for the disagreement in the vicinity of the first- and second-peak regions. A slight deviation is also found around the first minimum. The present authors maintain the view that these discrepancies arise mainly from the

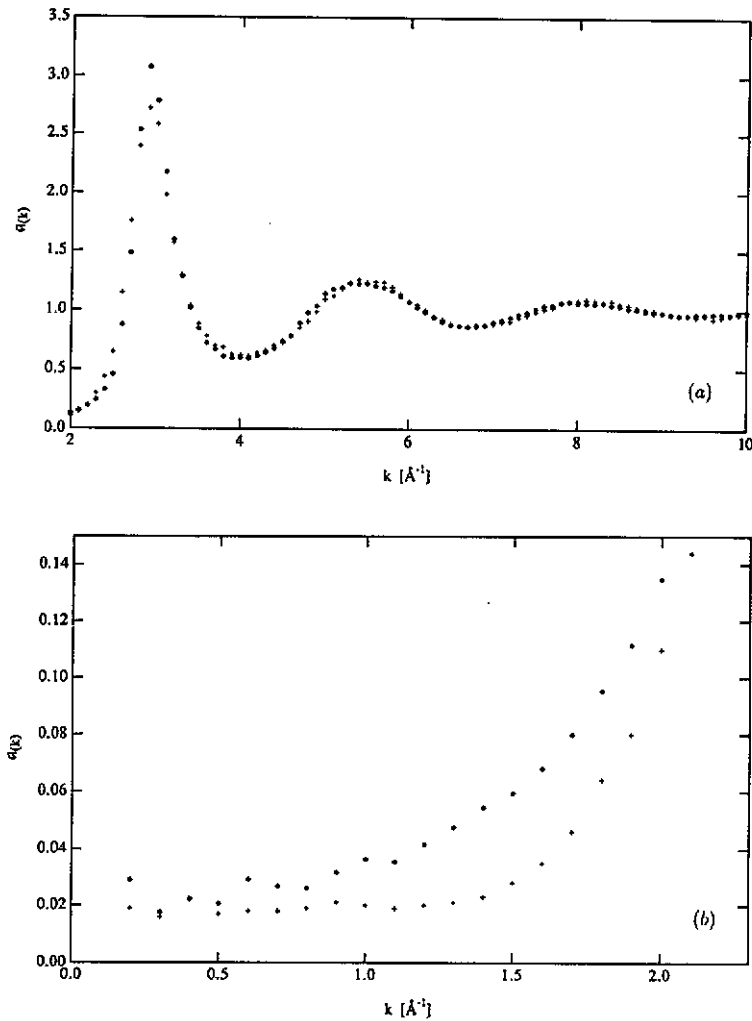


Figure 5. Structure factors of liquid Cu at 1423 K: +, for present potential; ◇, for first-principles interatomic potential (Lam *et al* 1983). (a) denotes the high- k region, and (b) the low- k region. The present results are obtained by averaging over 800 time steps.

choice of the $v_{\text{ref}}(r)$. For the low- k region the agreement between the calculated and experimental data is excellent and the degree of the agreement is seen from table 1. The potential of Lam *et al*, on the other hand, predicts too high a first peak and does not reproduce the low- k diffraction data although this potential does successfully describe the physical properties of solid Cu.

5.2. Pair distribution function

The calculated pair distribution functions $g(r)$ are displayed in figure 6 for comparison with experiment (Waseda 1980). The latter is obtained by Fourier transform of the experimental structure data. The calculated $g(r)$ are in good accord with experiment.

Table 1. Numerical details of structure factors below $k_0 (=2.384 \text{ \AA}^{-1})$. The present results are obtained by averaging over 800 time steps. The experimental data are due to Waseda and Ueno (1987).

$k (\text{\AA}^{-1})$	Expt	Present	$k (\text{\AA}^{-1})$	Expt	Present
0.1	0.0179	—	1.3	0.0223	0.021
0.2	0.0183	0.019	1.4	0.023	0.023
0.3	0.0185	0.016	1.5	0.027	0.028
0.4	0.0188	0.022	1.6	0.037	0.035
0.5	0.0192	0.017	1.7	0.043	0.046
0.6	0.0196	0.018	1.8	0.061	0.064
0.7	0.0201	0.018	1.9	0.076	0.080
0.8	0.0204	0.019	2.0	0.102	0.110
0.9	0.0209	0.021	2.1	0.139	0.144
1.0	0.0214	0.020	2.2	0.181	0.195
1.1	0.0216	0.019	2.3	0.231	0.299
1.2	0.0219	0.020			

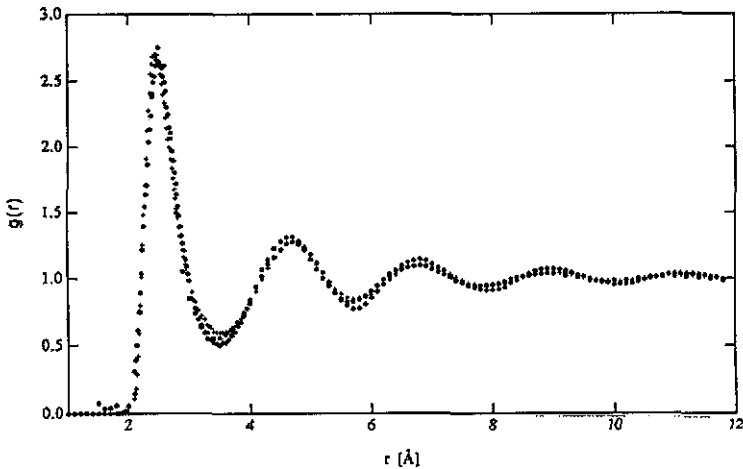


Figure 6. Comparison of pair distribution functions: ●, experiment (Waseda 1980); +, for present potential; ◇, for first-principles interatomic potential (Lam *et al* 1983).

However, it is seen in the case of the first-principles interatomic potential that there is a small phase shift in oscillation and this tends to be amplified with increasing distance.

Now we will focus on the second question: is this $v_{\text{eff}}(r)$ able to explain other physical properties than the liquid structure?

5.3. Specific heat at constant volume

It has been reported by González Miranda and Torra (1983) that the specific heat at constant volume C_V is rather insensitive to the details of the interatomic potential used.

Table 2. Comparison between the calculated and experimental C_V (Nk_B units). Electronic contribution to the specific heat ($\sim 0.1 Nk_B$) is included in the three calculated values.

	Present potential	Previous work ^a	Lam <i>et al</i> 's potential	Experiments
C_V	2.77	2.96	3.25	2.83 ^b (2.95) ^c

^a From Arai *et al* (1990a) in which $v_{\text{att}}(r)$ is not taken into account.

^b From Iida and Guthrie (1988).

^c From Hultgren *et al* (1973).

Table 3. Self-diffusion constant D ($10^{-9} \text{ m}^2 \text{ s}^{-1}$) and shear viscosity coefficient η (mPa) of liquid Cu at 1423 K.

	Present potential	Previous work ^a	Lam <i>et al</i> 's potential	Experiments ^b
D	3.91 (3.29)	2.55	2.50	3.97
η	3.00 (3.42)	4.34	—	3.2 ~ 4.34

^a From Arai *et al* (1990a) in which $v_{\text{att}}(r)$ is not taken into account.

^b From Iida and Guthrie (1988). These values are for the melting point.

(): Estimated values at the melting point (1356 K) using the formulae in the book of Iida and Guthrie.

However, we observe a small, though not significant, dependence of C_V on the potential used in the calculation. The calculated values of C_V are given in table 2.

5.4. Transport properties

Since a noteworthy sensitivity to $v_{\text{eff}}(r)$ may be detected in the atomic transport properties in liquid metals (Shimoji and Itami 1986) we have worked out self-diffusion constant D and shear viscosity coefficient η in order to examine the credibility of our $v_{\text{eff}}(r)$. In table 3, the calculated values of D and η are compared with the experimental values. As is remarked in the previous work on liquid Fe (Arai *et al* 1990b) both autocorrelation functions of the velocity and the stress tensor indicate the long-ranged oscillations, which makes it difficult to estimate errors in the calculated values. However, since the velocity autocorrelation function damps more quickly at the temperature near the melting point than that of the stress tensor we believe the calculated value of D is more reliable than the value of η . From table 3 we can see the transport properties are susceptible to the pair potential used in the calculation.

6. Conclusions

An effective pair potential $v_{\text{eff}}(r)$ for liquid Cu at 1423 K has been obtained from the small-angle structure factor data with the help of inverse power potentials to describe the structure factors in the high- k region. This $v_{\text{eff}}(r)$ indicates a marked difference, in position and depth of the first minimum, from the interatomic potential derived from first principles. A molecular dynamics calculation has been carried out in order to examine credibility of the present $v_{\text{eff}}(r)$. The following conclusions may be made.

(i) Using the present $v_{\text{eff}}(r)$ the experimental structure data, from well below the first peak to high k , can be reproduced by a molecular dynamics simulation.

(ii) The attractive and long-ranged part of the $v_{\text{eff}}(r)$ influences the height of the first peak (but not its location) and the low- k behaviour of the structure factor. The latter region is quite sensitive to the pair potential used.

(iii) The atomic transport properties are susceptible to the pair potential used as has been remarked by Shimoji and Itami (1986).

(iv) Many-ion interactions might be included in the present $v_{\text{eff}}(r)$ because it is extracted from the observed diffraction data. Such a factor may be one of the origins for the marked difference between the two potentials.

Acknowledgment

The authors are very grateful to Professor Y Waseda for a fruitful discussion of this work.

References

- Arai T, Yokoyama I and Waseda Y 1988 *J. Non-Cryst. Solids* **106** 104
 — 1990a *J. Non-Cryst. Solids* **117/118** 96
 — 1990b *High Temp. Mater. Proc.* **9** 51
 Berezhtkovsky L M, Drozdov A N, Zitserman V Y, Lagar'kov A N and Triger S A 1984 *J. Phys. F: Met. Phys.* **14** 2315
 Bratby P, Gaskell T and March N H 1970 *Phys. Chem. Liq.* **2** 53
 González Miranda J M and Torra V 1983 *J. Phys. F: Met. Phys.* **13** 281
 Hansen J P 1970 *Phys. Rev. A* **2** 221
 Hansen J P and McDonald I R 1986 *Theory of Simple Liquids* (London: Academic) pp 199, 267
 Hansen J P and Schiff D 1973 *Mol. Phys.* **25** 1281
 Hayter J B and Penfold J 1981 *Mol. Phys.* **42** 109
 Hayter J B, Pynn R and Suck J B 1983 *J. Phys. F: Met. Phys.* **13** L1
 Hoover W G, Gray S G and Johnson K W 1971 *J. Chem. Phys.* **55** 1128
 Hultgren R, Desai P D, Hawkins D T, Gleiser M, Kelly K K and Wagman D 1973 *Selected Values of the Thermodynamic Properties of the Elements* (Metals Park, OH: American Society of Metals) p 154
 Iida T and Guthrie R I L 1988 *The Physical Properties of Liquid Metals* (Oxford: Clarendon) pp 91, 174, 183, 185, 200, 211
 Johnson M D, Hutchinson P and March N H 1964 *Proc. R. Soc. A* **282** 283
 Johnson M D and March N H 1963 *Phys. Lett.* **3** 313
 Lam N Q, Dagens L and Doan N V 1983 *J. Phys. F: Met. Phys.* **13** 2503
 March N H 1987 *Can. J. Phys.* **65** 219
 — 1990 *Liquid Metals: Concepts and Theory* (Cambridge: Cambridge University Press) pp 39, 350
 March N H and Tosi M P 1976 *Atomic Dynamics in Liquids* (London: MacMillan) pp 78–84
 Naito S and Yokoyama I 1985 *J. Phys. F: Met. Phys.* **15** L295
 — 1988 *Z. Phys. Chem., NF* **156** 513
 — 1989 *High Temp. Mater. Proc.* **8** 251
 Shimoji M and Itami T 1986 *Atomic Transport in Liquid Metals* (Switzerland: Trans. Tech.) p 253
 Verlet L 1967 *Phys. Rev.* **159** 98
 Waseda Y 1980 *The Structure of Non-Crystalline Materials* (New York: McGraw-Hill) pp 264, 278
 Waseda Y and Ueno S 1987 *Sci. Rep. Res. Inst. Tohoku University* **34A** 15